










Highly efficient flame-retardant kraft paper

Fang Xu^{1,2} , Ling Zhong³ , Yuan Xu⁴ , Shaoyang Feng^{1,2} , Cheng Zhang^{1,2} , Fengxiu Zhang⁵ , and Guangxian Zhang^{1,2,*} 

¹ College of Textile and Garment, Southwest University, No. 2 Tiansheng Street, Beibei, Chongqing 400715, China

² Chongqing Engineering Research Center of Biomaterial Fiber and Modern Textile, Chongqing 400715, China

³ Chongqing Fibre Inspection Bureau, Chongqing 401121, China

⁴ College of Paper-making and Botanical Resources Engineering, Qilu University of Technology (Shandong Academy of Sciences), Jinan, Shandong 250353, China

⁵ Institute of Bioorganic and Medicinal Chemistry, College of Chemistry and Chemical Engineering, Southwest University, Chongqing 400715, China

Received: 12 June 2018

Accepted: 8 September 2018

Published online:

17 September 2018

© Springer Science+Business Media, LLC, part of Springer Nature 2018

ABSTRACT

The flame resistance of kraft paper was greatly modified by an eco-friendly, phosphorus-containing and reactive flame retardant, ammonium phosphite, which was grafted on kraft paper via pad-bake method. The results showed that the limiting oxygen index of treated kraft paper could increase from 19.1 to 48.2%. The results of vertical flammability tests imply that the char length of treated sample decreased from 210 to 45 mm. Thermogravimetry analysis showed that treated kraft paper had the lower initial decomposition temperature and more residues than control sample. Thermogravimetry analysis/infrared spectrometry indicated that the flammable volatile species of treated kraft paper reduced obviously compared with that of control sample. Fourier transform infrared spectroscopy suggested that ammonium phosphite was grafted on the cellulose molecules by P–O–C covalent bonds and the flame retardant is reactive in condensed phase. Scanning electron microscopy showed that the modification had little effect on the surface of kraft paper and the residual carbonized frame of treated kraft paper retained the fiber shape after combustion. EDX results showed that the flame retardant introduced a large amount of phosphorus and nitrogen into kraft paper. X-ray diffraction indicated that the modification did not significantly affect the crystal structure of kraft paper. And the strength of kraft papers slightly declined after the modification, but it still remained well.

Address correspondence to E-mail: zgx656472@sina.com

Introduction

Cellulosic paper is an important renewable resource and consists of cellulose, hemicelluloses and lignin [1–3]. It is widely used in packaging, construction, interior decoration, agriculture and daily necessities industries, due to its advantages of lightweight, low cost and so on [4, 5]. However, cellulosic paper is inherently flammable [6, 7]. It is easy to cause fire disasters, which seriously threaten human and their property [8]. Consequently, endowing paper with excellent flame retardancy to reduce the amount of fire disasters and expand the application scope of cellulosic paper is significant.

In recent years, researchers have suggested various methods and flame retardants to improve the flame-retardant property of cellulosic paper. According to these methods, the flame retardants can be classed to additive-type flame retardants and reactive flame retardants [9, 10].

Additive-type flame retardants are always directly added into papermaking pulp to produce flame-retardant paper. The main additive-type flame retardants are metal oxides, metal hydroxides, boron compounds and silicon compounds [11, 12]. These inorganic compounds have low flame-retardant efficiency. To enhance the flame retardancy of cellulosic paper, a large amount of inorganic compounds is needed, which is harmful to the physical properties of paper. In addition, some of them are heavy metal and will cause environmental pollution. So, some researchers added other highly effective flame retardants into papermaking pulp to produce synergies with these inorganic compounds [10, 13–15]. The synergistic effects of ammonium polyphosphate (APP)–diatomite–TiO₂ nanocomposites and APP–melamine cyanurate can reduce the mass loss of paper in combustion and make the residue more compact, and the LOI value can increase to about 30% [16–20]. Besides, some other organic flame retardants like poly(methylenephosphine) [21], guanidine phosphate [22] and guanidine sulfamate [23] are also used as fillers. But in practical applications, the method of adding flame retardants into papermaking pulp requires the flame retardants to meet some special requirements like good dispersibility, good filler retention, which restricts the use of some flame retardants.

In addition to adding flame retardants to the pulp directly, LbL assembly technique also has been

employed to deposit flame retardants onto pulp fibers or fabrics to improve the flame-retardant properties of paper [24–26]. Multilayered thin films of oppositely charged polyelectrolytes and/or nanoparticles were formed on the surface of fibers or fabrics via a multistep deposition process, attaching flame retardants to the surface fibers or fabrics. The dopants include cationic chitosan and anionic poly(vinylphosphonic acid) [24], cationic polyethylenimine and anionic sodium hexametaphosphate [25], polyaniline and phytic acid [26] and so on. This kind of methods has little damage to fibers and can reduce the flammable character of cellulosic fibers to some extent.

Reactive flame retardants including halogen-containing flame retardants, phosphorus-containing flame retardants and nitrogen-containing flame retardants are universally used by surface modification method [10]. Halogen compounds (chlorine-containing or bromine-containing) are widely used for paper and textile in the past. But these flame retardants will cause environmental pollution and pose a threat to human health, so they have been banned in European countries [27]. To develop efficient, non-toxic and eco-friendly flame retardants, phosphorus-containing flame retardants are used as substitutes for halogen flame retardants and often have synergistic effects with nitrogen-containing compounds. Some researchers impregnated paper with ammonium phosphate, monoammonium phosphate or diammonium phosphate solutions [28, 29]. It is found that these ammonium salts can graft on the cellulose by –P–O–C covalent bonds and the flame-retardant property of cellulosic paper was obviously improved. Using melamine formaldehyde and citric acid as crosslinking agents, N-hydroxymethyl-3-dimethylphosphonpropionamide was grafted on the surface of paper [30]. Besides, Tang and He et al. prepared flame-retardant paper using hexa(N-hydroxymethyl)amidocyclotriphosphazene and hexaamidocyclotriphosphazene, and these compounds play a flame retardant role mainly on condensed phase [31, 32]. However, some of these flame retardants containing hydroxymethyl will release carcinogenic formaldehyde in the modification and service process [27].

Phosphinates and hypophosphites like aluminum isobutylphosphinate [33], aluminum phenylphosphinate [34] and aluminum hypophosphite [35] were proven to be effectively flame retardants for

polyamides and polyester. During combustion, these flame retardants with high phosphorus-content can favor the formation of char to protect the surrounding polymer from further burning and decomposition. In this study, a high efficient, low-cost and environment-friendly reactive phosphite without halogens or formaldehyde, ammonium phosphite, was synthesized to improve the flame retardancy of kraft paper. The flame retardant was expected to graft on kraft paper by the reaction between $-OH$ groups of cellulose and $-PO(O^-NH_4^+)_2$ groups of ammonium phosphite. H_3PO_3 is more acidic than H_3PO_4 , so it is easier for ammonium phosphite to form anhydride and react with cellulose during the modification, and the finished kraft paper still well sustain flame retardancy after dipping in water for 24 h. The flame retardancy, thermal stability and combustion behavior were investigated comprehensively.

Experimental

Materials

Kraft paper with a weight of 120 g/m^2 was purchased from Southwest University Culture Supermarket in Chongqing, China. Phosphorous acid (H_3PO_3), urea and ammonium hydroxide were purchased from Chengdu Kelong Chemical Reagent Co., Ltd. (Chengdu, China). Dicyandiamide was supplied by Aladdin Reagent Co., Ltd. (Shanghai, China). All reagents were used as received without any purification.

Synthesis of $(NH_4)_2HPO_3$ solution

Phosphorous acid (**1**, 24.6 g, 0.300 mol), urea (**2**, 18 g, 0.300 mol) and distilled water (100 mL) were added into a 250-mL three-necked, round-bottomed flask. The mixed solution was heated up to $110\text{ }^\circ\text{C}$ in the nitrogen atmosphere (with a flow rate of 20 mL/min) under magnetic stirring using a thermostatic heating magnetic stirrer (CL-2, Zhengzhou, China). The temperature was held at $110\text{ }^\circ\text{C}$ for 60 min and then heated up to $125\text{ }^\circ\text{C}$ for 10 min. After that, the pH was adjusted to about 6 by ammonium hydroxide and the crude product (**3**) was subsequently obtained. Finally, the product was purified by precipitation using anhydrous ethanol, filtered, dried at

$60\text{ }^\circ\text{C}$ and the white solid of ammonium phosphite was obtained. This synthetic route is shown in Scheme 1a.

Flame-retardant finishing of kraft paper

Different concentrations of ammonium phosphite solutions (5, 10, 15, 20, 25 and 30%) were prepared by dissolving ammonium phosphite in distilled water. And dicyandiamide as catalyst was added to the solutions at a mass concentration of 5%. Then, the samples of kraft paper (size $20\text{ cm} \times 20\text{ cm}$) were immersed into the mixed solutions at $60\text{ }^\circ\text{C}$ for 10 min with a bath ratio of 1:20. (The bath ratio is the kraft paper weight *versus* the volume of the solution.) Subsequently, the samples were padded through a nip to reach wet pickup of about 120%. After that, the samples were cured at $150\text{ }^\circ\text{C}$ for 5 min in an automatic continuous baking machine (Mini-Tentr, Xiamen Rapid Co. Ltd., China). Finally, the finished samples were washed with distilled water and dried in an oven at $60\text{ }^\circ\text{C}$. The possible reaction between $(NH_4)_2HPO_3$ and cellulose is presented in Scheme 1b, and the process illustration of the flame retardant modification is shown in Fig. 1. The weight gain (WG) was calculated using the following formula:

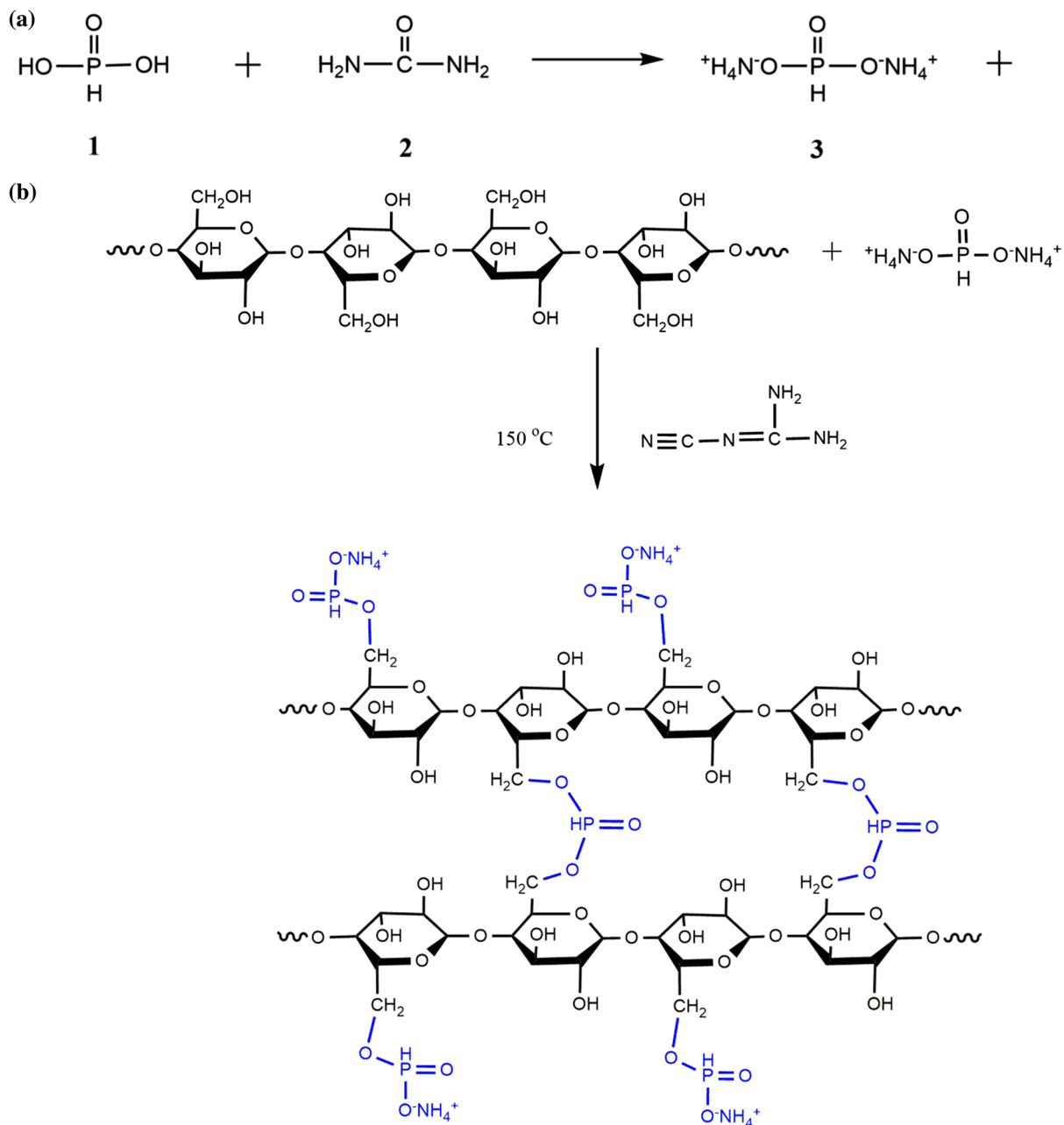
$$WG (\%) = \frac{W_1 - W_0}{W_0} \times 100\% \quad (1)$$

where W_0 is the weight of control kraft paper and W_1 is the weight of treated kraft paper.

Characterization

LOI tests were performed with a digital display oxygen index instrument M606B (Qingdao Shanfang Instrument Co. Ltd., China) based on the ASTM D2863-2000 standard test method. The LOI values of control and modified kraft papers were conducted. Besides, the LOI values of modified kraft paper after dipping in water were measured. The modified kraft papers were dipped in water at room temperature for 24 h and then dried at $60\text{ }^\circ\text{C}$.

Vertical flammability tests were carried out according to TAPPI T461OS-79 testing procedure using YG815B vertical fabric flame-retardant tester (Nantong Sansi Electromechanical Science & Technology Co. Ltd., China). And the samples used in this test were of $70\text{ mm} \times 210\text{ mm}$.



Scheme 1 Synthetic route of $(\text{NH}_4)_2\text{HPO}_3$ (a), and reaction between cellulose and $(\text{NH}_4)_2\text{HPO}_3$ (b).

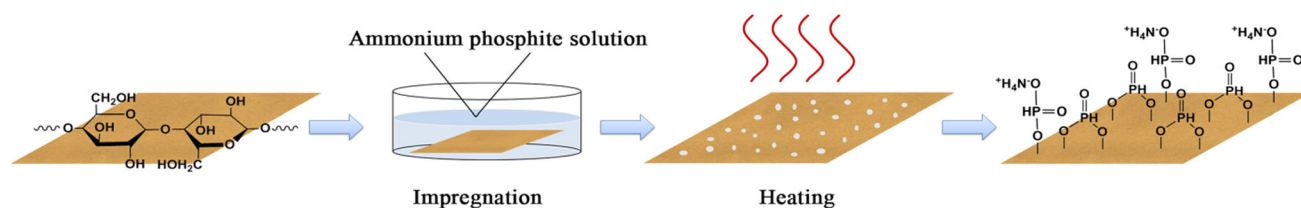


Figure 1 Process illustration of the flame retardant modification for kraft paper.

The surface morphologies of control, treated and the burnt kraft papers were observed using a Hitachi

S-4800 field emission scanning electron microscopy instrument (Netherlands). The samples were coated

with a thin layer of gold using a GSL-1100X-SPC-16 M magnetron plasma sputtering coater (MTI Corporation, USA). And the elemental compositions were determined with an energy-dispersive X-ray spectroscopy (EDX) (China).

FTIR spectra of kraft papers and char residues were obtained using a Spectrum GX spectrometer (PE Co., USA) in the range of 400–4000 cm^{-1} , with a resolution of 4 cm^{-1} . Before the tests, kraft paper samples were cut into powder and mixed with KBr in a ratio of 1:100.

The crystalline structures of kraft papers were investigated using a D/max-B X-ray diffraction diffractometer (Rigaku Co., Japan) with Cu $K\alpha$ radiation generated at 36 kV and 20 mA. The angle was from 5° to 50° in steps of 0.02° ($\lambda = 0.154$ nm). The degree of crystallinity and crystalline dimension of kraft paper were calculated according to the following equations:

$$\text{Cr} (\%) = \frac{S_e}{S_e + S_n} \times 100\% \quad (2)$$

where Cr denotes degree of crystallinity and S_e and S_n denote the area of the crystalline peak and the noncrystalline peak, respectively.

$$L_{hkl} = \frac{K\lambda}{\beta \cos \theta} \quad (3)$$

where L_{hkl} denotes the crystallite size; K stands for the Scherrer constant taken as 0.9; and β stands for the width (in radians) at the half height of the characteristic diffraction peak.

TG analysis of kraft papers was investigated using a Pyris 1 thermogravimetric analyzer (Perkin-Elmer, USA). The samples (8.5 ± 0.5 mg) were tested in the range of 40–700 °C with a heating rate of 10 °C/min and in the nitrogen atmosphere with a flow rate of 60 mL/min.

A Pyris 1 thermogravimetric analyzer (Perkin-Elmer, USA) coupled with a Nicolet 6700 FTIR spectrophotometer through a transfer pipe was used to obtain the TG-IR analysis spectra of kraft papers. The samples were tested under a nitrogen atmosphere with a heating rate of 10 °C/min from 40 to 700 °C, and the flow rate of nitrogen atmosphere was 60 mL/min.

The tensile index and strain at break of control and treated kraft papers were measured using an electromechanical universal testing machine (MTS SYSTEMS Co., Ltd., China) according to ISO 1924-2:2008.

The samples (15 mm × 180 mm) were tested using constant rate of elongation method (20 mm/min).

Results and discussion

Flame resistance

LOI and vertical flame tests were conducted to investigate the flame resistance of kraft papers. The corresponding results from these tests are shown in Table 1 and Fig. 2.

Table 1 lists the LOI values, WG and the vertical flammability test data of control kraft paper (KP) and treated kraft papers (KP-5, KP-10, KP-15, KP-20, KP-25, KP-30). It can be seen that LOI values increase distinctly following the increase in $(\text{NH}_4)_2\text{HPO}_3$ concentration. LOI value of control kraft paper is only 19.1%. By contrast, KP-5 shows a LOI value of 26.5% (LOI > 26, not burn in normal atmosphere) with a flame-retardant rating of B-1, and KP-10 shows a flame-retardant rating of B-0. When the concentration of $(\text{NH}_4)_2\text{HPO}_3$ solution increases to 30%, the LOI value reaches 48.2%. After dipping in water at room temperature for 24 h, the LOI values of treated kraft papers decreased. But the LOI values still sustain above 26% when the concentration of $(\text{NH}_4)_2\text{HPO}_3$ is above 20%, and the flame resistance is well maintained.

According to Table 1 and Fig. 2, the treated kraft papers show excellent flame-retardant properties. The control kraft paper sample burns out completely and vigorously in air, with 3 s of after-flame time, and no residues left after combustion. After modification, all kraft papers have no after-flame or after-glow time; these samples stop the propagation of flame immediately when the flame is removed. Meanwhile, large quantities of char are obviously left in the igniting area. For KP-5, KP-10, KP-15, KP-20, KP-25, KP-30, the char lengths are 84, 72, 58, 52, 50 and 45 mm, and the weight gain values are 3.6, 6.7, 10.5, 12.9, 16.8 and 23.7%, respectively. These results verify that the modification can endow kraft paper with high flame-retardant efficiency, with no release of halogens or formaldehyde. It is likely that flame retardant is reactive in condensed phase and has the efficiency in altering combustion characteristics and favoring the formation of carbonaceous char.

Table 1 LOI values, WG and vertical flammability test results of control and treated kraft paper samples

Samples	Concentration of FR (%)	Weight gain (%)	After-flame time (s)	After-glow time (s)	Char length (mm)	LOI (%)	Rating ^a	LOI after dipping (%)
KP	0	–	3 ± 1	0	No residues	19.1	NR	–
KP-5	5	3.6 ± 0.9	0	0	82 ± 4	26.5	B-1	21.9
KP-10	10	6.7 ± 0.7	0	0	72 ± 2	35.8	B-0	24.7
KP-15	15	10.5 ± 1.0	0	0	58 ± 3	40.2	B-0	25.8
KP-20	20	12.9 ± 0.5	0	0	52 ± 2	44.6	B-0	26.5
KP-25	25	16.8 ± 0.7	0	0	50 ± 2	46.5	B-0	28.3
KP-30	30	23.7 ± 0.5	0	0	45 ± 2	48.2	B-0	29.9

^a(B-0: non-inflammable, LOI > 35; B-1: difficultly flammable, 25 < LOI ≤ 35; B-2: flammable, 20 < LOI ≤ 25). [22]

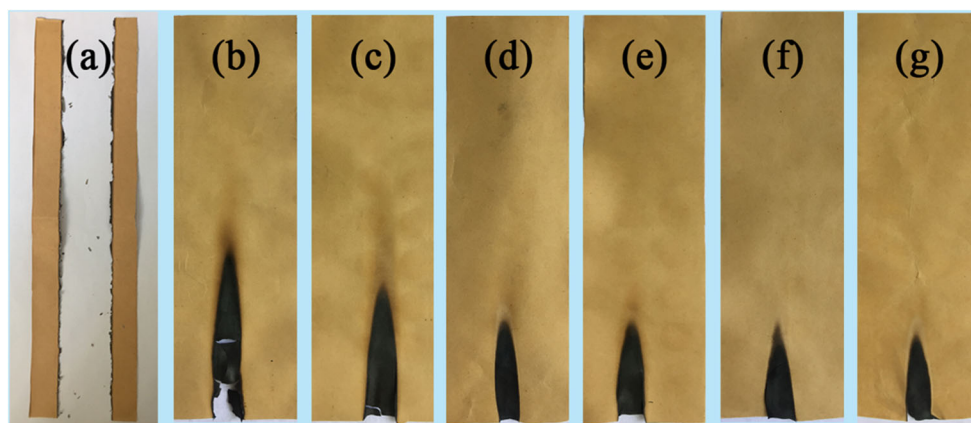


Figure 2 Pictures of KP (a), KP-5 (b), KP-10 (c), KP-15 (d), KP-20 (e), KP-25 (f) and KP-30 (g) after vertical flammability tests.

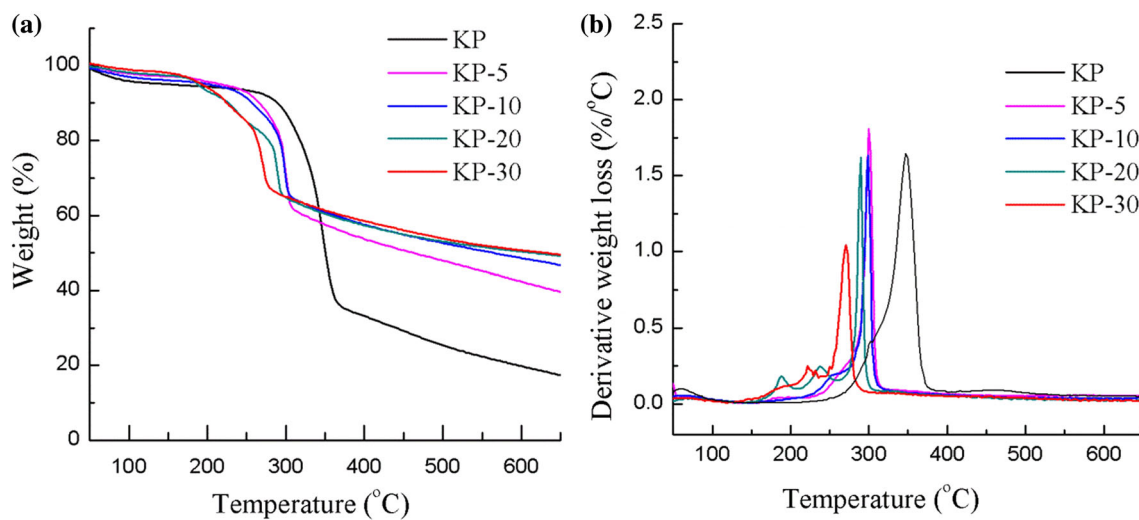


Figure 3 TG (a) and DTG (b) curves of KP, KP-5, KP-10, KP-15, KP-20, KP-25 and KP-30 in nitrogen atmosphere.

Table 2 TG data of kraft paper samples under nitrogen atmosphere

Samples	$T_{\text{onset}10\%}$ (°C)	T_{max} (°C)	CY ₆₀₀ (%)
KP	288.2	347.5	19.8
KP-5	266.1	299.7	42.1
KP-10	256.9	299.4	48.6
KP-20	227.4	289.9	50.3
KP-30	225.2	270.6	50.7

Thermal stability

The thermal stabilities of control and treated kraft papers were evaluated by TG in nitrogen atmosphere; the curves of TG and DTG are shown in Fig. 3 (a) and (b), respectively. And the data of TG and DTG, such as the 10 wt% mass loss temperature ($T_{10\%}$), the temperature at maximum mass loss rate (T_{max}) and char yield at 600 °C (CY₆₀₀), are summarized in Table 2.

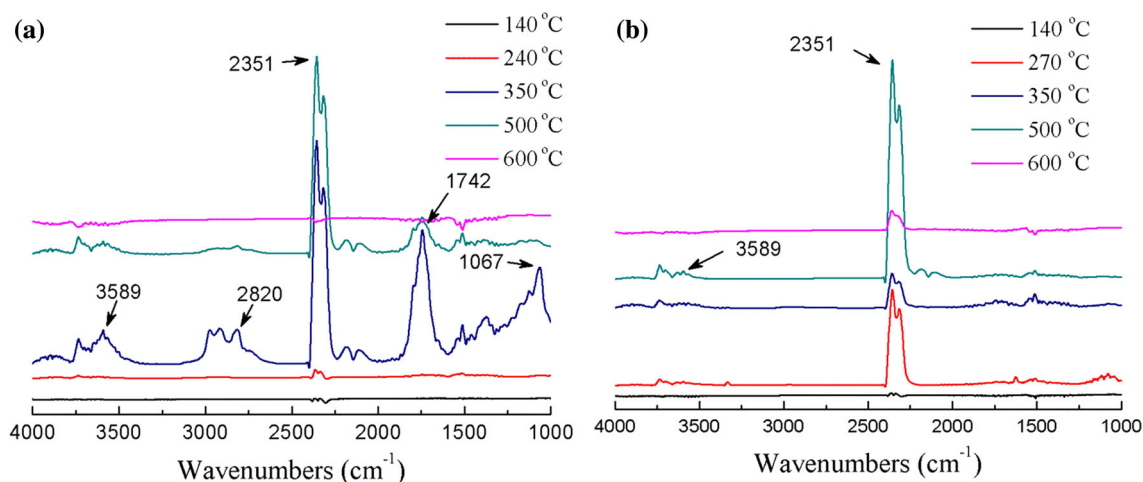
As shown in Fig. 3 (a), the control kraft paper has the $T_{10\%}$ at 288.2 °C and T_{max} at 347.5 °C, which corresponds to the depolymerization of the glycosyl units to volatile products involves levoglucosan [27]. With the increase of temperature, the control kraft paper has the CY₆₀₀ of 19.8%. Compared with control kraft paper, the treated kraft papers have lower $T_{10\%}$, lower T_{max} and more residues. In addition, $T_{10\%}$ and T_{max} decrease with the increase of (NH₄)₂HPO₃ concentration, and CY₆₀₀ increases with the increase of

(NH₄)₂HPO₃ concentration. The $T_{10\%}$ reduction is due to the decomposition of flame retardant and the evolution of ammonia and water as gaseous products between 200 and 400 °C. In the meantime, P–O–P or P–N–P bonds are formed resulting in ultraphosphate structures [36]. When the concentration of (NH₄)₂HPO₃ increases to 30%, the CY₆₀₀ increases to 50.7%, which is 156.06% higher than that of control kraft paper. The results demonstrate that the modification can endow kraft paper with high thermal stability. The flame retardant catalyzes the dehydration of kraft paper, favoring the formation of carbonaceous char and preventing the depolymerization of cellulose [23, 27, 37, 38].

TG-IR analysis

TG-IR was employed to investigate the changes of gaseous volatiles released from kraft papers during thermal degradation, and explore the thermal degradation mechanism of kraft paper.

The FTIR spectra of pyrolysis products from KP and KP-30 at different temperatures are shown in Fig. 4. During thermal degradation, the gaseous pyrolysis products of control kraft paper mainly exhibit characteristic signals peaks (Fig. 4a): vibration absorption of –OH from water vapor at 3589 cm⁻¹, absorption of aliphatic C–H bond from diverse alkanes at 2820 cm⁻¹, absorption of CO₂ at 2351 cm⁻¹, stretching vibration absorption of C=O group at 1742 cm⁻¹, and the stretching vibration of

**Figure 4** FTIR spectra of pyrolysis products of kraft papers at different temperatures: **a** KP, **b** KP-30.

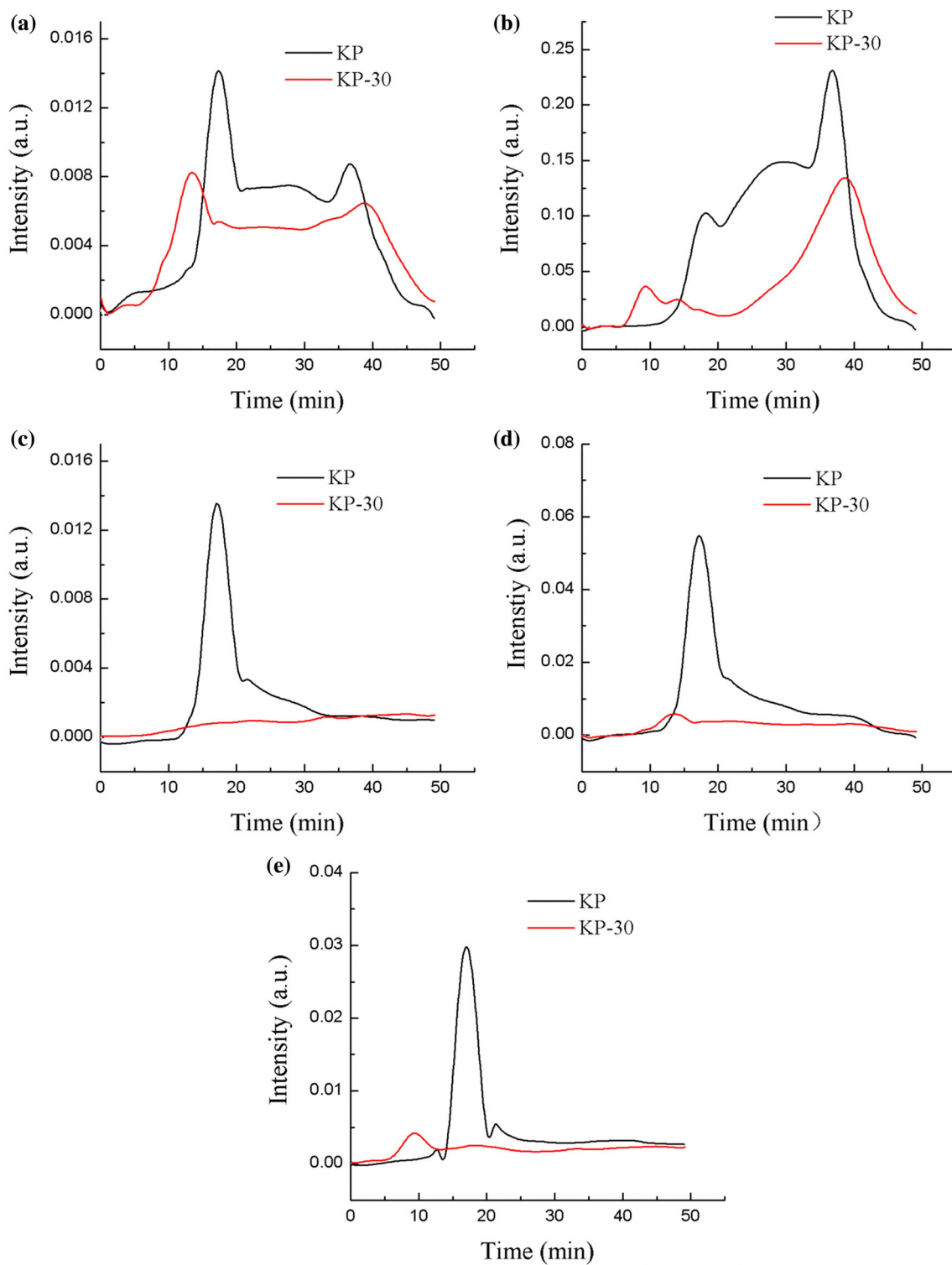


Figure 5 Intensities of characteristic peaks for pyrolysis products of KP and KP-30: **a** H₂O, **b** CO₂, **c** hydrocarbons, **d** carbonyl compounds and **e** ethers.

C–O–C bond from ethers at 1067 cm^{-1} . Among them, water vapor and CO₂ are non-flammable volatile species; hydrocarbons, carbonyl compounds and

ethers belong to flammable ones. From Fig. 4b, KP-30 does not show new absorption peaks compared with KP. And KP-30 mainly releases a small amount of the

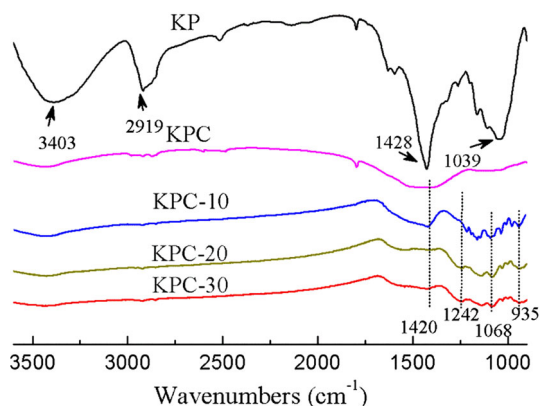


Figure 6 FTIR spectra of control kraft paper (KP), carbonized control kraft paper (KPC) and carbonized treated kraft paper samples (KPC-10, KPC-20 and KPC-30).

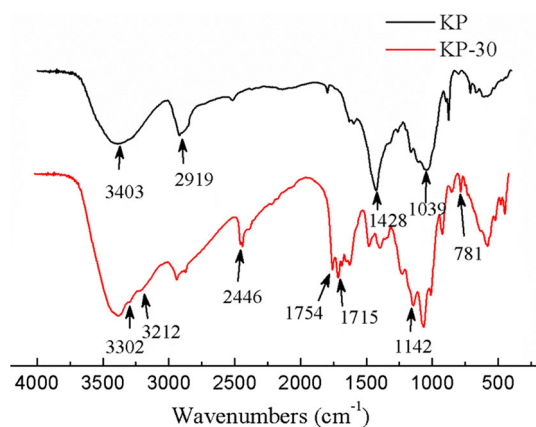


Figure 7 FTIR spectra of KP and KP-30.

non-flammable water vapor and CO_2 during the thermal degradation.

The intensity of characteristic peaks for main gaseous pyrolysis products of KP and KP-30 is shown in Fig. 5a–e, to further study the effect of modification on thermal degradation process. All the maximum absorption intensities of these gaseous pyrolysis products reduce after the modification, especially the flammable gaseous pyrolysis products. These results indicate that the flame retardant can favor the decomposition of glycosyl units to form carbonaceous char, instead of releasing volatile products. In addition, the time of treated kraft paper started to pyrolysis is earlier than control kraft paper, and the same phenomenon is shown in Fig. 4a and b. This result indicates that grafted flame retardant can decrease the initial decomposition temperature, which agrees with the results of TG analysis.

FTIR analysis

To further disclose the flame-retardant mechanism in the condensed phase, the FTIR of kraft papers and char residues was investigated (the char residue of KP, KP-10, KP-20 and KP-30 are labeled KPC, KPC-10, KPC-20 and KPC-30, respectively), and the results are shown in Fig. 6. KP has the main absorption peaks at 3403, 2919, 1428 and 1039 cm^{-1} , which are the characteristic peaks of cellulose. The peak at 3403 cm^{-1} is assigned to $-\text{OH}$ stretching vibration absorption, a peak at 2919 cm^{-1} is assigned to $\text{C}-\text{H}$ absorption, a peak at 1428 cm^{-1} is assigned to $\text{C}-\text{C}$ absorption, and a peak at 1039 cm^{-1} is assigned to $\text{C}-\text{O}-\text{C}$ bonds absorbing. As can be seen in the figure, the peaks almost disappear for carbonized kraft paper samples (KPC, KPC-10, KPC-20 and KPC-30), except the $\text{C}-\text{C}$ absorption at 1420 cm^{-1} . And the spectra of KPC-10, KPC-20 and KPC-30 show some new peaks at 1242, 1068 and 935 cm^{-1} . The peak at 1242 cm^{-1} corresponds to the vibration absorption of $\text{P}=\text{O}$, the peak at 1068 cm^{-1} is ascribed to $\text{P}-\text{N}$ stretching vibration from the NH_3 decomposed by $(\text{NH}_4)_2\text{HPO}_3$ reacting with the $\text{P}=\text{O}$ bond. The peak at 935 cm^{-1} is attributed to $\text{P}-\text{O}-\text{P}$ stretching vibrations, which indicates the dehydration of the $\text{P}-\text{OH}$ groups and the formation of polyphosphoric acid. During combustion, $\text{H}_3\text{PO}_3/\text{H}_3\text{PO}_4$ and polyphosphoric acid are produced which promoted the char layer formation of kraft paper. The dense char layer can hinder heat and mass transfer between gas and condensed phases and protect kraft paper from further oxidation.

FTIR was also employed to investigate the chemical structures of kraft paper before and after the modification and verify the reaction between $(\text{NH}_4)_2\text{HPO}_3$ and cellulose of kraft paper. The FTIR spectra of KP and KP-30 are shown in Fig. 7. Both KP and KP-30 have some characteristic peaks of cellulose. Compared with KP, KP-30 has some new peaks at 781, 1142, 1715, 1754, 2446, 3212 and 3302 cm^{-1} . The peak at 781 cm^{-1} corresponds to $\text{P}-\text{O}-\text{C}$ absorption, the peak at 1142 cm^{-1} corresponds to the vibration absorption of $\text{P}=\text{O}$, and the peak at 2446 cm^{-1} is assigned to $\text{P}-\text{H}$ absorption. The results indicate that the flame retardant is grafted on the kraft paper by forming $\text{P}-\text{O}-\text{C}$ bond. The peaks at 3212 and 3302 cm^{-1} correspond to the vibration absorption of NH_4^+ units. In addition, the peak at 1715 and 1754 cm^{-1} is assigned to the $\text{C}=\text{O}$

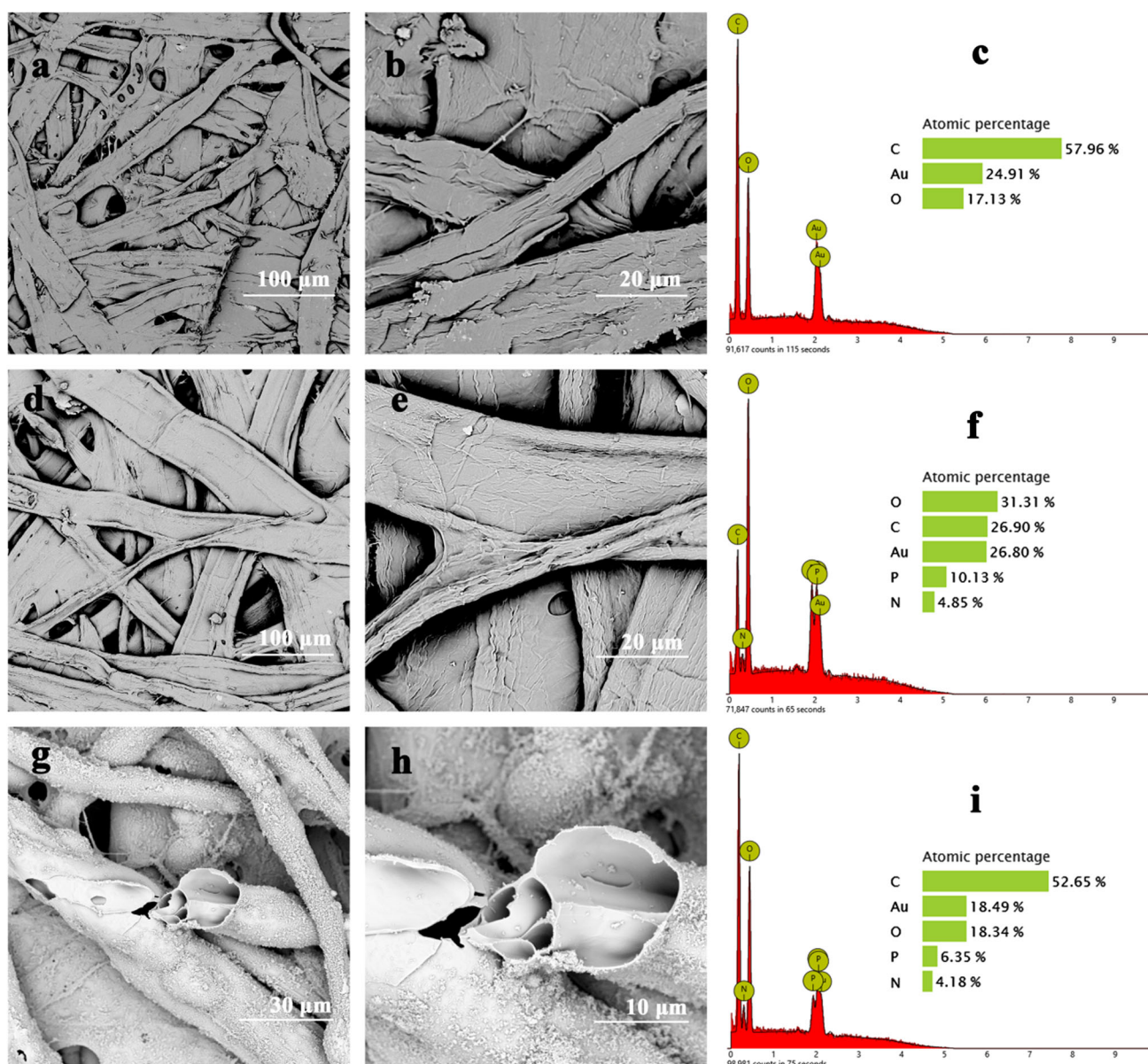


Figure 8 SEM images and EDX results of kraft papers. KP (a–c), KP-30 (d–f) and burnt KP-30 (g–i). The magnification times were 800 in a, d; 3000 in b, e; 2500 in g; and 6000 in h.

stretching vibration, which is probably because a small amount of oxidation occurs during the modification.

Surface morphology and elemental constitution

SEM was used to observe the surface micromorphologies of KP, KP-30 and KPC-30, and the images are shown in Fig. 8. As shown in Fig. 8 a and b, the fibers of KP are flat and disorganized with rough surface and curly edges. The curly edges of fibers are

maintained in KP-30 (Fig. 8 d and e), and the fibers of KP-30 are smoother than the fibers of KP, with a little swollen. These results demonstrate that $(\text{NH}_4)_2\text{HPO}_3$ can enter the interior of fibers and reacts with cellulose molecules, causing fibers to become swollen. The images of KPC-30 are shown in Fig. 8 g and h. After combustion, a large amount of carbon residue of treated kraft paper is markedly remained. The puffy and dense char layer is formed, and the residual carbonized frame retains the fiber shape. These results verify the efficiency of the flame retardant in favoring the formation of char.

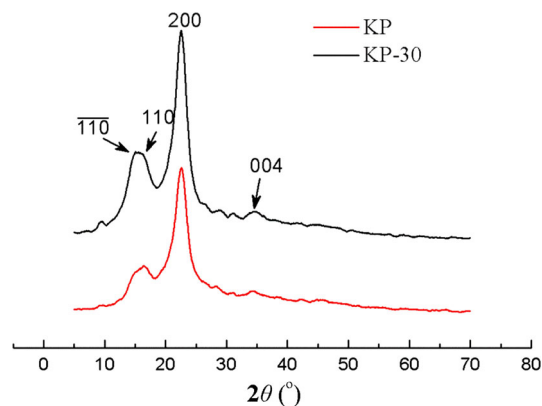


Figure 9 XRD spectra of KP and KP-30.

The chemical composition on the surface of KP, KP-30 and KPC-30 was investigated by EDX test, and the results are shown in Fig. 8. As shown in Fig. 8 c, only C and O are detected in KP. And the obvious P and N signals are newly obtained in KP-30, which indicate that the modification can endow kraft paper with high P and N element content, with the obvious increase in O element content. In KPC-30, the O element content decreases a lot because the dehydration reaction of kraft paper during combustion. However, a great amount of P and N element are remained. It means that the nonvolatile phosphides are formed and some N-containing compounds are combined with P to form P-N structure during combustion,

which agrees with the results of FTIR. The non-volatile phosphides in condensed phase can favor the formation of char and increase the barrier property of chars to hinder heat, oxygen and flammable gases transfer between gas and condensed phases.

X-ray diffraction analysis

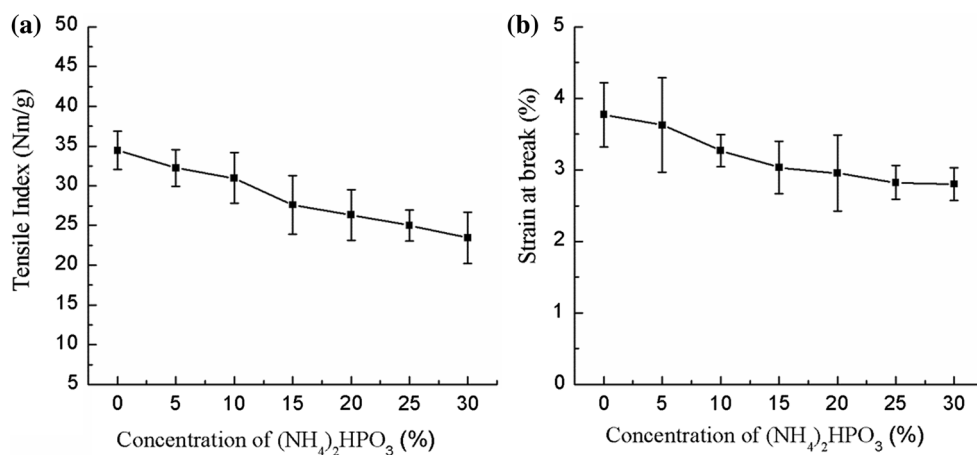
XRD was used to investigate the crystal structures of the control and treated kraft papers. Figure 9 shows the X-ray diffraction spectra of KP and KP-30. From the spectra, it can be concluded that control kraft paper shows the main diffraction peaks at $2\theta = 14.7^\circ$, 16.2° , 22.6° and 34.2° , corresponding to the $(\bar{1}10)$, (110) , (200) and (004) crystallographic planes of characteristics diffraction peaks of cellulose I [39–42]. This result shows that the main component of the control kraft paper is cellulose I. The spectrum of KP-30 is similar to that of KP. There is almost no change in diffraction angles of characteristic peaks, indicating that the flame-retardant modification does not significantly affect the crystal structure of kraft paper.

The degree of crystallinity and crystalline dimension of kraft paper were calculated using Eqs. 2 and 3, respectively, and the related parameters are shown in Table 3. The degree of crystallinity of KP-30 (48.49%) decreases slightly, compared with that of KP (52.56%). For the crystalline dimension, there is no

Table 3 Crystal parameters of KP and KP-30

Samples	Degree of crystallinity (%)	Crystalline dimension (nm)			
		$\bar{1}10$	110	200	004
KP	52.56	2.89	4.28	3.48	3.39
KP-30	48.49	2.46	4.55	3.48	3.95

Figure 10 Tensile index (a) and strain at break values (b) for control and treated kraft papers.



obvious change observed between control and treated kraft papers. These results indicate that the modification does not significantly affect the degree of crystallinity and crystallite size of kraft paper.

Strength properties

Figure 10 shows the tensile index and strain at break of control and treated kraft papers. From Fig. 10a and b, it can be seen that the tensile index and strain at break of kraft paper decrease gradually as the $(\text{NH}_4)_2\text{HPO}_3$ concentration increases. The tensile index of the control kraft paper is 34.456 Nm/g, whereas the tensile index of KP-30 is 23.465 Nm/g, 31.89% lower. This is possible because that the temperature and flame retardant have some influence on the strength properties of kraft papers during the modification. Even so, the tensile index of treated kraft paper is still high enough to meet the requirements in many fields.

Conclusions

In this work, a highly efficient and eco-friendly reactive flame retardant, ammonium phosphite, was synthesized for kraft paper. During the modification, the $-\text{PO}(\text{O}^-\text{NH}_4^+)_2$ groups of ammonium phosphite reacted with $-\text{OH}$ groups of cellulose to form P–O–C covalent bond, which made the flame retardant firmly graft on fibers of kraft paper. From the results, this reactive flame-retardant exhibited excellent flame resistance for kraft paper with LOI value of 48.2%, and the flame resistance was well maintained after dipping in water for 24 h. During decomposition, the grafted flame retardant decomposed to catalyze the dehydration of kraft paper and favored the formation of carbonaceous char instead of releasing volatile products. The flame retardant is cost-efficient and easily synthesized, and the modification is facile and efficient. Therefore, this reactive phosphite flame retardant for kraft paper can be used in a wide range of applications.

Acknowledgement

This work was supported by the “Fundamental Research Funds for the Central Universities” (Grant No. XDJK2018D009).

References

- [1] Kazuaki N, Megumi A, Takayuki T et al (2018) Lignocellulose nanofibers prepared by ionic liquid pretreatment and subsequent mechanical nanofibrillation of bagasse powder: application to esterified bagasse/polypropylene composites. *Carbohydr Polym* 182:8–14
- [2] Francisco MJ, Estrada RHC, Carrillo JG (2018) Water absorption and termite attack on a kraft paper-based composite treated with recycled polystyrene and three commercial resins. *Eur J Wood Wood Prod* 76:469–479
- [3] Pereira CS, Silveira RL, Dupree P et al (2017) Effects of xylan side-chain substitutions on xylan-cellulose interactions and implication for thermal pretreatment of cellulosic biomass. *Biomacromol* 18:1311–1321
- [4] Dong LY, Zhu YJ (2017) A new kind of fireproof, flexible, inorganic, nanocomposite paper and its application to the protection layer in flame-retardant fiber-optic cables. *Chem Eur J* 23:4597–4604
- [5] Messmer NR, Guerrini LM, Oliveira MP (2018) Effect of unmodified kraft lignin concentration on the emulsion and miniemulsion copolymerization of styrene with n-butyl acrylate and methacrylic acid to produce polymer hybrid latex. *Polym Adv Technol* 29:1094–1106
- [6] Lee S, Teramoto Y, Shiraishi N (2002) Biodegradable polyurethane foam from liquefied waste paper and its thermal stability, biodegradability, and genotoxicity. *J Appl Polym Sci* 83(7):1482–1489
- [7] Basak S, Samanta KK, Chattopadhyay SK et al (2015) Thermally stable cellulosic paper made using banana pseudostem sap, a wasted by-product. *Cellulose* 22:2767–2776
- [8] Basak S, Patil PG, Shaikh AJ et al (2016) Green coconut shell extract and boric acid: new formulation for making thermally stable cellulosic paper. *Cellulose* 91:2871–2881
- [9] Shen J, Song ZQ, Qian XR et al (2011) A review on use of fillers in cellulosic paper for functional applications. *Ind Eng Chem Res* 50:661–666
- [10] Wag SL, Huang JL, Chen FS (2012) Study on Mg–Al hydrotalcites in flame-retardant paper preparation. *BioResources* 7(1):997–1007
- [11] Si YF, Guo ZG (2016) Eco-friendly functionalized superhydrophobic recycled paper with enhanced flame-retardancy. *J Colloid Interface Sci* 477:74–82
- [12] Mo ZY, Zhao HF, Wu CL et al (2016) Resin microencapsulated ammonium polyphosphate. *Paper Paper Making* 35(7):35–38
- [13] Li XH, Qian XR (2008) Application of Mg–Al hydrotalcite as flame-retardant filler in papermaking. *China Pulp Paper* 27(12):16–19

- [14] An XH, Qian XR, Long YF (2007) Preparation of flame retardant paper based on in situ synthesis of Mg-Al hydroxalates. *China Pulp Paper* 26(8):1–5
- [15] Nassar MM, Fadali OA, Khattab MA et al (1999) Thermal studies on paper treated with flame-retardant. *Fire Mater* 23:125–129
- [16] Zhao HF, Sha LZ (2017) Synergistic effect of nano-TiO₂, ammonium polyphosphate and diatomite ternary system on flame retardancy and smoke suppression of filled paper. *Dig J Nanomater Biostruct* 12(2):473–481
- [17] Lin H, Sha LZ, Zhao HF (2017) Synthesis of ammonium polyphosphate/diatomite composite filler and its effect on the flame retardancy of paper. *Paper Paper Making* 36(2):30–33
- [18] Sha LZ, Chen KF (2014) Preparation and characterization of ammonium polyphosphate/diatomite composite fillers and assessment of their flame-retardant effects on paper. *BioResources* 9(2):3104–3116
- [19] Sha LZ, Chen KF (2016) Surface modification of ammonium polyphosphate-diatomaceous earth composite filler and its application in flame-retardant paper. *J Therm Anal Calorim* 123:339–347
- [20] Yang WG, Yang F, Yang RD et al (2016) Ammonium polyphosphate/melamine cyanurate synergetic flame retardant system for use in papermaking. *BioResources* 11(1):2308–2318
- [21] Prieger AM, Siu PW, Hu TQ et al (2015) Flammability properties of paper coated with poly(methylenephosphine), an organophosphorus polymer. *Fire Mater* 39:647–657
- [22] Wang N, Liu YS, Liu Y et al (2017) Properties and mechanisms of different guanidine flame retardant wood pulp paper. *J Anal Appl Pyrol* 128:224–231
- [23] Wang N, Liu YS, Xu CG et al (2017) Acid-base synergistic flame retardant wood pulp paper with high thermal stability. *Carbohydr Polym* 178:123–130
- [24] Koklukaya O, Carosio F, Grunlan JC et al (2015) Flame-retardant paper from wood fibers functionalized via layer-by-layer assembly. *ACS Appl Mater Interfaces* 7:23750–23759
- [25] Koklukaya O, Carosio F, Wagberg L (2018) Tailoring flame-retardancy and strength of papers via layer-by-layer treatment of cellulose fibers. *Cellulose* 25:2691–2709
- [26] Zhou Y, Ding CY, Qian XR et al (2015) Further improvement of flame retardancy of polyaniline-deposited paper composite through using phytic acid as dopant or co-dopant. *Carbohydr Polym* 115:670–676
- [27] Jia YL, Lu Y, Zhang GX et al (2017) Facile synthesis of an eco-friendly nitrogen-phosphorus ammonium salt to enhance the durability and flame retardancy of cotton. *J Mater Chem A* 5:9970–9981
- [28] Ilia G, Drehe M, Iliescu S et al (2011) Flame retardants based on phosphoric acid for wood, textiles and paper. *Rev Chim* 62(12):1141–1144
- [29] Candan Z, Ayrlimis N, Dundar T (2012) Fire performance of LVL panels treated with fire retardant chemicals. *Wood Res* 57(4):651–658
- [30] Katović D, Bischof VS, Flinčec GS et al (2009) Flame retardancy of paper obtained with environmentally friendly agents. *Fib Text Eastern Eur* 17(3):90–94
- [31] He W, Bi W, Yang K et al (2015) Flame retarded paper prepared with hexaamidocyclotriphosphazene. *Paper Sci Technol* 34(4):24–26
- [32] Tang LS, Zhao J, Sui XT et al (2016) Impact of the mixture of hexa(N-hydroxymethyl)amidocyclotriphosphazene and partially methylated melamine formaldehyde resin on the flame retardancy of paper. *Fib Text Eastern Eur* 24(4):153–160
- [33] Zhao B, Chen L, Long JW et al (2013) Synergistic effect between aluminum hypophosphite and alkyl-substituted phosphinate in flame-retarded polyamide 6. *Ind Eng Chem Res* 52:17162–17170
- [34] Zhao B, Chen L, Long JW et al (2013) Aluminum hypophosphite versus alkyl-substituted phosphinate in polyamide 6: flame retardance, thermal degradation, and pyrolysis behavior. *Ind Eng Chem Res* 52:2875–2886
- [35] Zhao B, Hu Z, Chen L et al (2011) A phosphorus-containing inorganic compound as an effective flame retardant for glass-fiber-reinforced polyamide 6. *J Appl Polym Sci* 119:2379–2385
- [36] Davies PJ, Horrocks AR, Alderson A (2005) The sensitization of thermal decomposition of ammonium polyphosphate by selected metal ions and their potential for improved cotton fabric flame retardancy. *Polym Degrad Stab* 88:114–122
- [37] Gao WW, Zhang GX, Zhang FX (2015) Enhancement of flame retardancy of cotton fabrics by grafting a novel organic phosphorous-based flame retardant. *Cellulose* 22:2787–2796
- [38] Feng YJ, Zhou Y, Li DK et al (2017) A plant-based reactive ammonium phytate for use as a flame-retardant for cotton fabric. *Carbohydr Polym* 175:636–644
- [39] Espinosa E, Sánchez R, Otero R et al (2017) A comparative study of the suitability of different cereal straws for lignocelluloses nanofibers isolation. *Int J Biol Macromol* 103:990–999
- [40] Bumbudsanpharoke N, Ko S (2018) The green fabrication, characterization and evaluation of catalytic antioxidation of gold nanoparticle-lignocellulose composite papers for active packaging. *Int J Biol Macromol* 107:1782–1791
- [41] Kafle K, Lee CM, Shin H et al (2015) Effects of delignification on crystalline cellulose in lignocelluloses biomass characterized by vibrational sum frequency generation

spectroscopy and X-ray diffraction. *Bioenergy Res* 8:1750–1758

[42] Goodell B, Zhu Y, Kim S et al (2017) Modification of the nanostructure of lignocelluloses cell walls via a non-

enzymatic lignocelluloses deconstruction system in brown rot wood-decay fungi. *Biotechnol Biofuels* 10:179